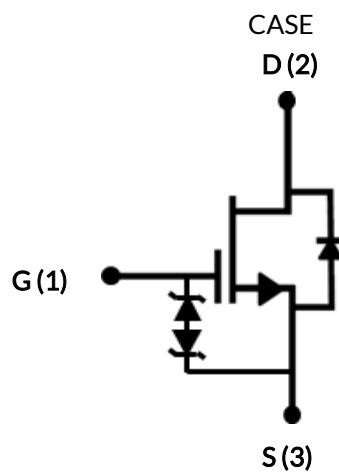
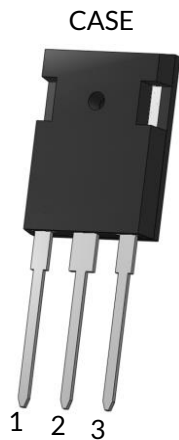


## DATASHEET

# UJ4C075060K3S



## 750V-58mΩ SiC FET

Rev. A, October 2020

### Description

The UJ4C075060K3S is a 750V, 58mΩ G4 SiC FET. It is based on a unique ‘cascode’ circuit configuration, in which a normally-on SiC JFET is co-packaged with a Si MOSFET to produce a normally-off SiC FET device. The device’s standard gate-drive characteristics allows for a true “drop-in replacement” to Si IGBTs, Si FETs, SiC MOSFETs or Si superjunction devices. Available in the TO-247-3L package, this device exhibits ultra-low gate charge and exceptional reverse recovery characteristics, making it ideal for switching inductive loads and any application requiring standard gate drive.

### Features

- ◆ On-resistance  $R_{DS(on)}$ : 58mΩ (typ)
- ◆ Operating temperature: 175°C (max)
- ◆ Excellent reverse recovery:  $Q_{rr}$  = 52nC
- ◆ Low body diode  $V_{FSD}$ : 1.31V
- ◆ Low gate charge:  $Q_G$  = 37.8nC
- ◆ Threshold voltage  $V_{G(th)}$ : 4.8V (typ) allowing 0 to 15V drive
- ◆ Low intrinsic capacitance
- ◆ ESD protected, HBM class 2

Part Number	Package	Marking
UJ4C075060K3S	TO-247-3L	UJ4C075060K3S

### Typical applications

- ◆ EV charging
- ◆ PV inverters
- ◆ Switch mode power supplies
- ◆ Power factor correction modules
- ◆ Motor drives
- ◆ Induction heating



## Maximum Ratings

Parameter	Symbol	Test Conditions	Value	Units
Drain-source voltage	$V_{DS}$		750	V
Gate-source voltage	$V_{GS}$	DC	-20 to +20	V
Continuous drain current <sup>1</sup>	$I_D$	$T_C = 25^\circ\text{C}$	28	A
		$T_C = 100^\circ\text{C}$	20.6	A
Pulsed drain current <sup>2</sup>	$I_{DM}$	$T_C = 25^\circ\text{C}$	62	A
Single pulsed avalanche energy <sup>3</sup>	$E_{AS}$	$L=15\text{mH}, I_{AS}=1.8\text{A}$	24.3	mJ
Power dissipation	$P_{tot}$	$T_C = 25^\circ\text{C}$	155	W
Maximum junction temperature	$T_{J,max}$		175	$^\circ\text{C}$
Operating and storage temperature	$T_J, T_{STG}$		-55 to 175	$^\circ\text{C}$
Max. lead temperature for soldering, 1/8" from case for 5 seconds	$T_L$		250	$^\circ\text{C}$

1. Limited by  $T_{J,max}$

2. Pulse width  $t_p$  limited by  $T_{J,max}$

3. Starting  $T_J = 25^\circ\text{C}$

## Thermal Characteristics

Parameter	Symbol	Test Conditions	Value			Units
			Min	Typ	Max	
Thermal resistance, junction-to-case	$R_{\theta JC}$			0.75	0.97	$^\circ\text{C}/\text{W}$

## Electrical Characteristics ( $T_J = +25^\circ\text{C}$ unless otherwise specified)

### Typical Performance - Static

Parameter	Symbol	Test Conditions	Value			Units
			Min	Typ	Max	
Drain-source breakdown voltage	$BV_{DS}$	$V_{GS}=0V, I_D=1mA$	750			V
Total drain leakage current	$I_{DSS}$	$V_{DS}=750V, V_{GS}=0V, T_J=25^\circ\text{C}$		0.7	40	$\mu\text{A}$
		$V_{DS}=750V, V_{GS}=0V, T_J=175^\circ\text{C}$		15		
Total gate leakage current	$I_{GSS}$	$V_{DS}=0V, T_J=25^\circ\text{C}, V_{GS}=-20V / +20V$		4.7	$\pm 20$	$\mu\text{A}$
Drain-source on-resistance	$R_{DS(on)}$	$V_{GS}=12V, I_D=20A, T_J=25^\circ\text{C}$		58	74	m $\Omega$
		$V_{GS}=12V, I_D=20A, T_J=125^\circ\text{C}$		106		
		$V_{GS}=12V, I_D=20A, T_J=175^\circ\text{C}$		147		
Gate threshold voltage	$V_{G(th)}$	$V_{DS}=5V, I_D=10mA$	4	4.8	6	V
Gate resistance	$R_G$	f=1MHz, open drain		4.5		$\Omega$

### Typical Performance - Reverse Diode

Parameter	Symbol	Test Conditions	Value			Units
			Min	Typ	Max	
Diode continuous forward current <sup>1</sup>	$I_S$	$T_C=25^\circ\text{C}$			28	A
Diode pulse current <sup>2</sup>	$I_{S,pulse}$	$T_C=25^\circ\text{C}$			62	A
Forward voltage	$V_{FSD}$	$V_{GS}=0V, I_F=10A, T_J=25^\circ\text{C}$		1.31	1.75	V
		$V_{GS}=0V, I_F=10A, T_J=175^\circ\text{C}$		1.8		
Reverse recovery charge	$Q_{rr}$	$V_R=400V, I_F=20A, V_{GS}=0V, R_{G,EXT}=20\Omega$		52		nC
Reverse recovery time	$t_{rr}$	$di/dt=1060A/\mu\text{s}, T_J=25^\circ\text{C}$		16		ns
Reverse recovery charge	$Q_{rr}$	$V_R=400V, I_F=20A, V_{GS}=0V, R_{G,EXT}=20\Omega$		58		nC
Reverse recovery time	$t_{rr}$	$di/dt=1060A/\mu\text{s}, T_J=150^\circ\text{C}$		19		ns

## Typical Performance - Dynamic

Parameter	Symbol	Test Conditions	Value			Units	
			Min	Typ	Max		
Input capacitance	$C_{iss}$	$V_{DS}=100V, V_{GS}=0V$ $f=100kHz$		1422		pF	
Output capacitance	$C_{oss}$			68			
Reverse transfer capacitance	$C_{rss}$			2.7			
Effective output capacitance, energy related	$C_{oss(er)}$	$V_{DS}=0V$ to 400V, $V_{GS}=0V$		50		pF	
Effective output capacitance, time related	$C_{oss(tr)}$	$V_{DS}=0V$ to 400V, $V_{GS}=0V$		94		pF	
$C_{oss}$ stored energy	$E_{oss}$	$V_{DS}=400V, V_{GS}=0V$		4		$\mu J$	
Total gate charge	$Q_G$	$V_{DS}=400V, I_D=20A,$ $V_{GS} = 0V$ to 15V		37.8		nC	
Gate-drain charge	$Q_{GD}$			8			
Gate-source charge	$Q_{GS}$			11.8			
Turn-on delay time	$t_{d(on)}$	Note 4, $V_{DS}=400V, I_D=20A,$ Gate Driver =0V to +15V, Turn-on $R_{G,EXT}=1\Omega,$ Turn-off $R_{G,EXT}=20\Omega$ Inductive Load, FWD: same device with $V_{GS} = 0V, R_G = 20\Omega,$ $T_J=25^\circ C$		13		ns	
Rise time	$t_r$			29			
Turn-off delay time	$t_{d(off)}$			78			
Fall time	$t_f$			13			
Turn-on energy	$E_{ON}$			168			
Turn-off energy	$E_{OFF}$		58		$\mu J$		
Total switching energy	$E_{TOTAL}$		226				
Turn-on delay time	$t_{d(on)}$	Note 4, $V_{DS}=400V, I_D=20A,$ Gate Driver =0V to +15V, Turn-on $R_{G,EXT}=1\Omega,$ Turn-off $R_{G,EXT}=20\Omega$ Inductive Load, FWD: same device with $V_{GS} = 0V, R_G = 20\Omega,$ $T_J=150^\circ C$		13		ns	
Rise time	$t_r$			31			
Turn-off delay time	$t_{d(off)}$			84			
Fall time	$t_f$			14			
Turn-on energy	$E_{ON}$			189			
Turn-off energy	$E_{OFF}$			70			$\mu J$
Total switching energy	$E_{TOTAL}$			259			

4. Measured with the half-bridge mode switching test circuit in Figure 28.

## Typical Performance - Dynamic (continued)

Parameter	Symbol	Test Conditions	Value			Units	
			Min	Typ	Max		
Turn-on delay time	$t_{d(on)}$	Note 5, $V_{DS}=400V$ , $I_D=20A$ , Gate Driver =0V to +15V, $R_{G,EXT}=1\Omega$ , inductive Load, FWD: same device with $V_{GS}=0V$ and $R_G=1\Omega$ , RC snubber: $R_{S1}=10\Omega$ and $C_{S1}=95pF$ , $T_J=25^\circ C$		13		ns	
Rise time	$t_r$			31			
Turn-off delay time	$t_{d(off)}$			31			
Fall time	$t_f$			9			
Turn-on energy including $R_S$ energy	$E_{ON}$		Note 5, $V_{DS}=400V$ , $I_D=20A$ , Gate Driver =0V to +15V, $R_{G,EXT}=1\Omega$ , inductive Load, FWD: same device with $V_{GS}=0V$ and $R_G=1\Omega$ , RC snubber: $R_{S1}=10\Omega$ and $C_{S1}=95pF$ , $T_J=25^\circ C$		186		$\mu J$
Turn-off energy including $R_S$ energy	$E_{OFF}$				18		
Total switching energy	$E_{TOTAL}$				204		
Snubber $R_S$ energy during turn-on	$E_{RS\_ON}$				0.5		
Snubber $R_S$ energy during turn-off	$E_{RS\_OFF}$				0.9		
Turn-on delay time	$t_{d(on)}$	Note 5, $V_{DS}=400V$ , $I_D=20A$ , Gate Driver =0V to +15V, $R_{G,EXT}=1\Omega$ , inductive Load, FWD: same device with $V_{GS}=0V$ and $R_G=1\Omega$ , RC snubber: $R_{S1}=10\Omega$ and $C_{S1}=95pF$ , $T_J=150^\circ C$		13		ns	
Rise time	$t_r$			35			
Turn-off delay time	$t_{d(off)}$			34			
Fall time	$t_f$			10			
Turn-on energy including $R_S$ energy	$E_{ON}$		Note 5, $V_{DS}=400V$ , $I_D=20A$ , Gate Driver =0V to +15V, $R_{G,EXT}=1\Omega$ , inductive Load, FWD: same device with $V_{GS}=0V$ and $R_G=1\Omega$ , RC snubber: $R_{S1}=10\Omega$ and $C_{S1}=95pF$ , $T_J=150^\circ C$		210		$\mu J$
Turn-off energy including $R_S$ energy	$E_{OFF}$				24		
Total switching energy	$E_{TOTAL}$				234		
Snubber $R_S$ energy during turn-on	$E_{RS\_ON}$				0.5		
Snubber $R_S$ energy during turn-off	$E_{RS\_OFF}$				0.9		
Turn-on delay time	$t_{d(on)}$	Note 6, $V_{DS}=400V$ , $I_D=20A$ , Gate Driver = 0V to +15V, Turn-on $R_{G,EXT}=1\Omega$ , Turn-off $R_{G,EXT}=20\Omega$ Inductive Load, FWD: UJ3D06510TS $T_J=25^\circ C$		13		ns	
Rise time	$t_r$			26			
Turn-off delay time	$t_{d(off)}$			78			
Fall time	$t_f$			12		$\mu J$	
Turn-on energy	$E_{ON}$			142			
Turn-off energy	$E_{OFF}$			56			
Total switching energy	$E_{TOTAL}$			198			
Turn-on delay time	$t_{d(on)}$	Note 6, $V_{DS}=400V$ , $I_D=20A$ , Gate Driver =0V to +15V, Turn-on $R_{G,EXT}=1\Omega$ , Turn-off $R_{G,EXT}=20\Omega$ Inductive Load, FWD:UJ3D06510TS $T_J=150^\circ C$		13		ns	
Rise time	$t_r$			30			
Turn-off delay time	$t_{d(off)}$			83			
Fall time	$t_f$			15			
Turn-on energy	$E_{ON}$			162		$\mu J$	
Turn-off energy	$E_{OFF}$			70			
Total switching energy	$E_{TOTAL}$			232			

5. Measured with the chopper mode switching test circuit in Figure 30.

6. Measured with the chopper mode switching test circuit in Figure 29.

## Typical Performance Diagrams

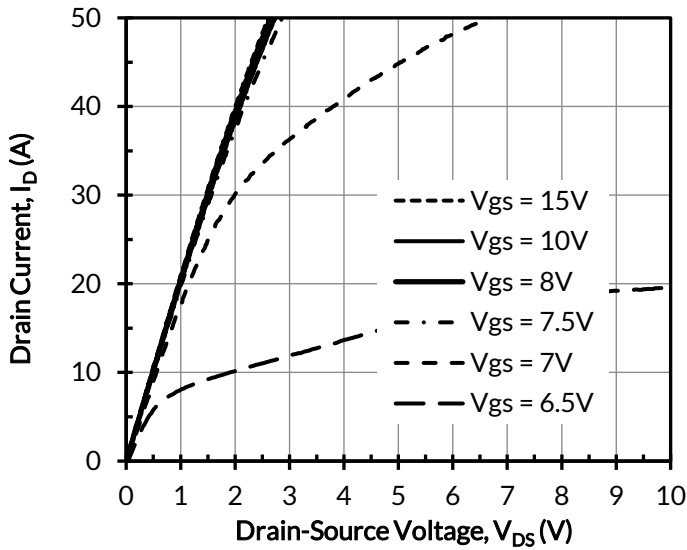


Figure 1. Typical output characteristics at  $T_j = -55^\circ\text{C}$ ,  $t_p < 250\mu\text{s}$

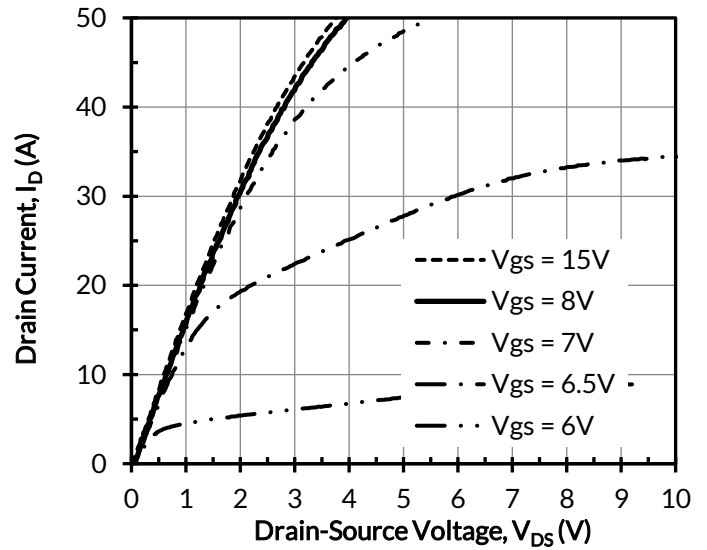


Figure 2. Typical output characteristics at  $T_j = 25^\circ\text{C}$ ,  $t_p < 250\mu\text{s}$

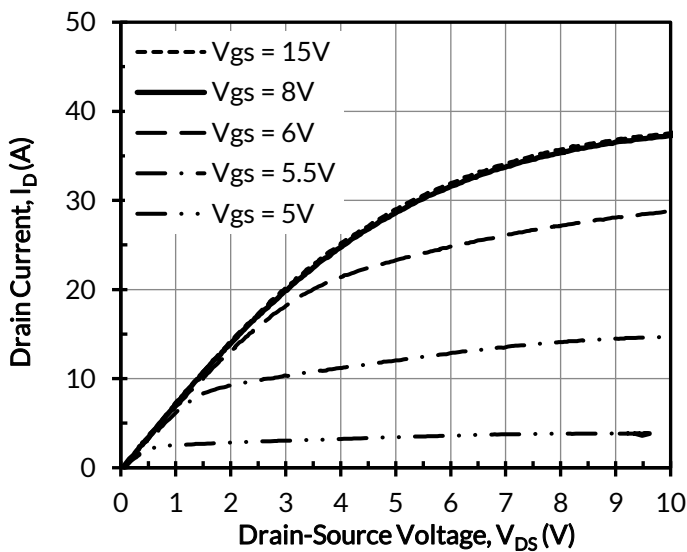


Figure 3. Typical output characteristics at  $T_j = 175^\circ\text{C}$ ,  $t_p < 250\mu\text{s}$

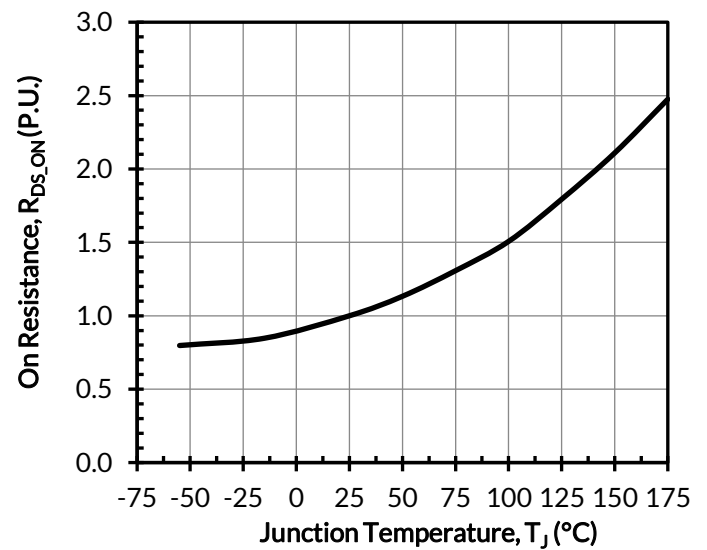


Figure 4. Normalized on-resistance vs. temperature at  $V_{GS} = 12\text{V}$  and  $I_D = 20\text{A}$

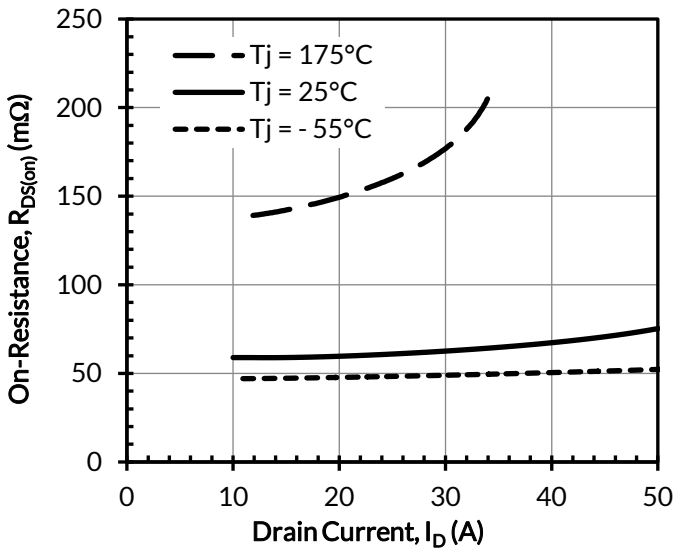


Figure 5. Typical drain-source on-resistances at  $V_{GS} = 12\text{V}$

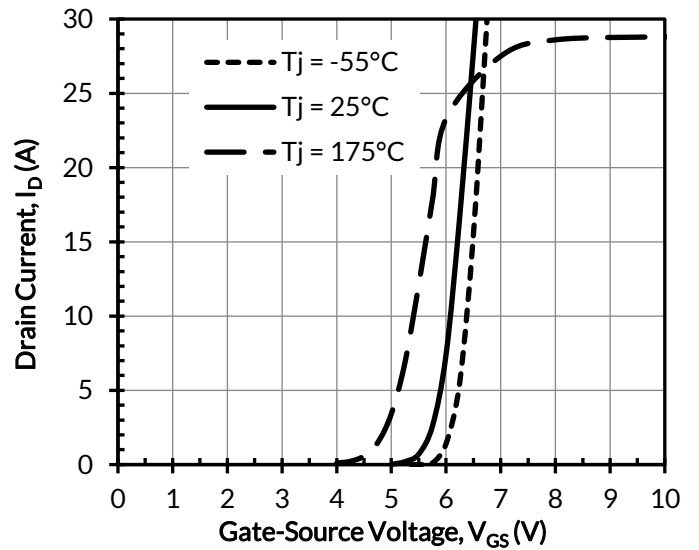


Figure 6. Typical transfer characteristics at  $V_{DS} = 5\text{V}$

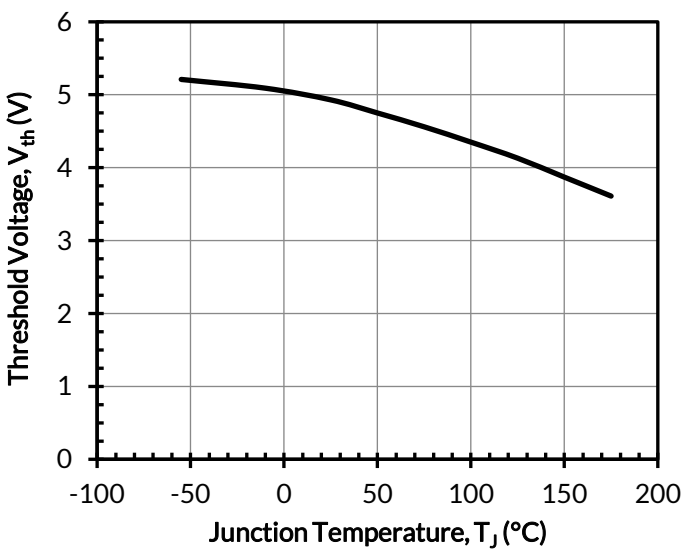


Figure 7. Threshold voltage vs. junction temperature at  $V_{DS} = 5\text{V}$  and  $I_D = 10\text{mA}$

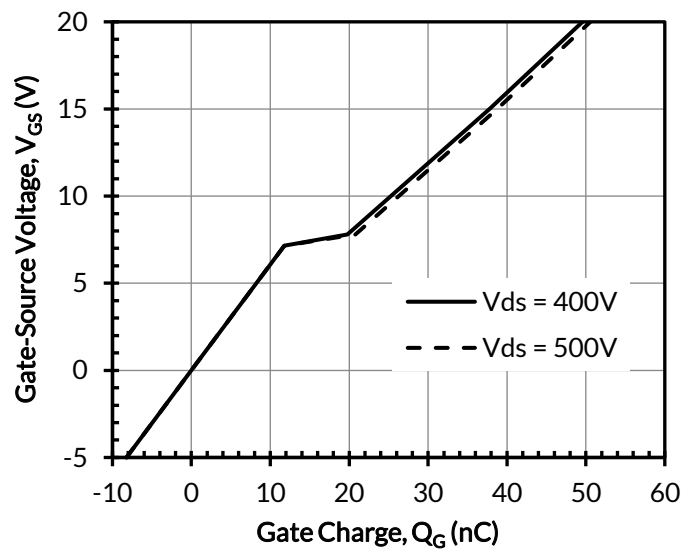


Figure 8. Typical gate charge at  $I_D = 20\text{A}$

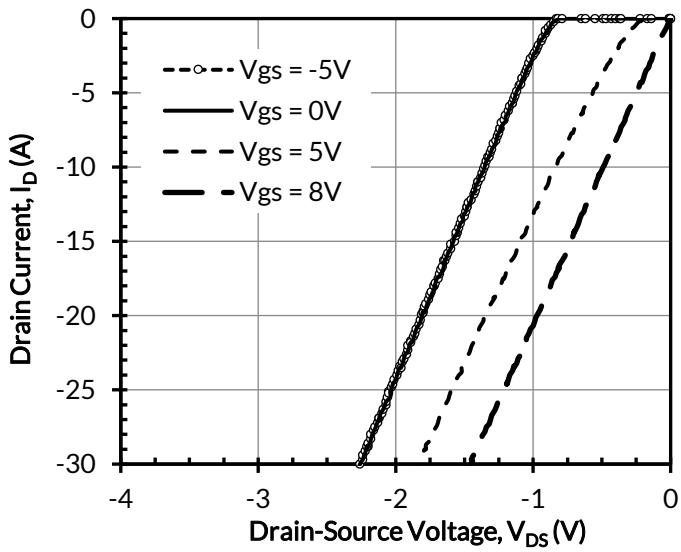


Figure 9. 3rd quadrant characteristics at  $T_j = -55^\circ\text{C}$

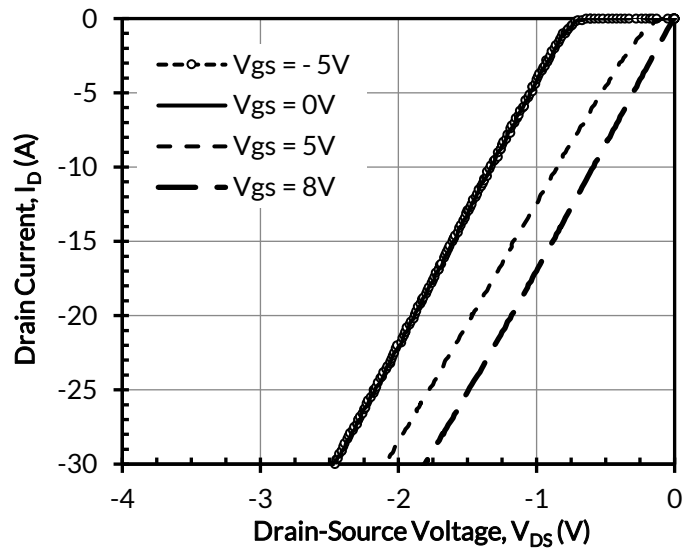


Figure 10. 3rd quadrant characteristics at  $T_j = 25^\circ\text{C}$

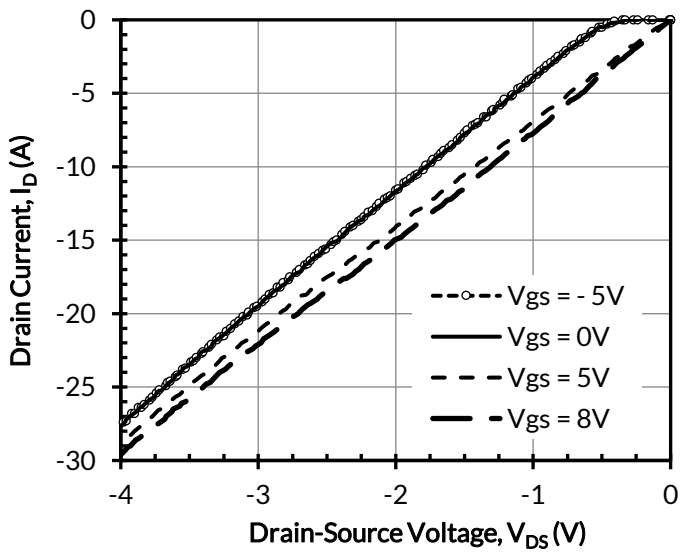


Figure 11. 3rd quadrant characteristics at  $T_j = 175^\circ\text{C}$

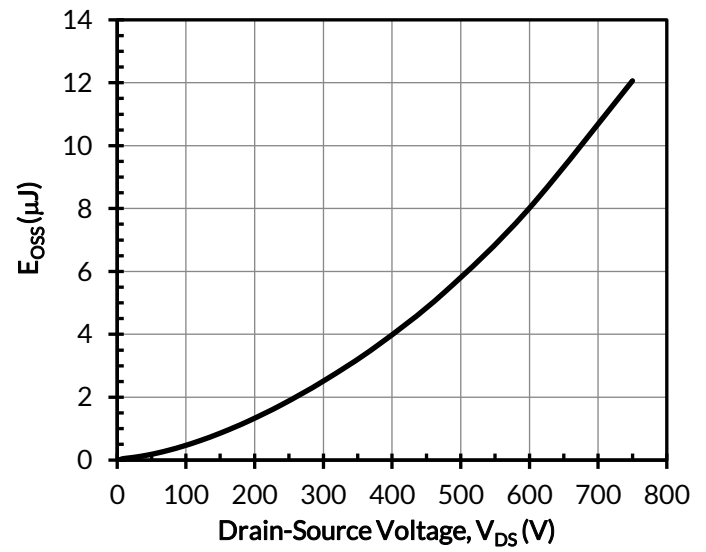


Figure 12. Typical stored energy in  $C_{OSS}$  at  $V_{GS} = 0\text{V}$



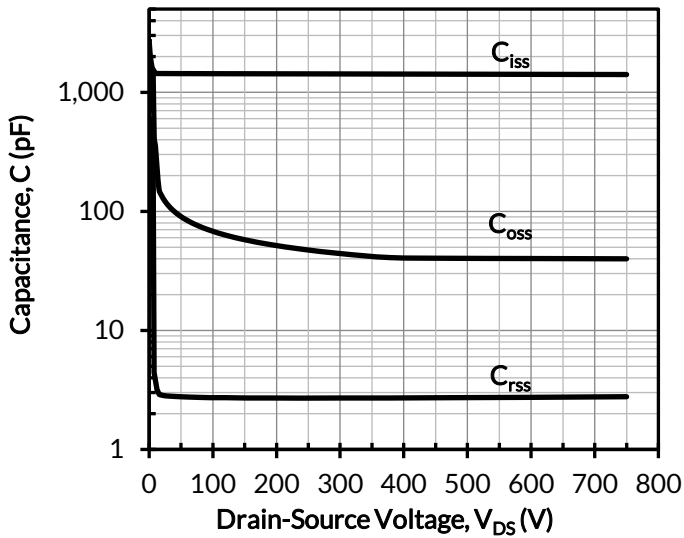


Figure 13. Typical capacitances at  $f = 100\text{kHz}$  and  $V_{GS} = 0\text{V}$

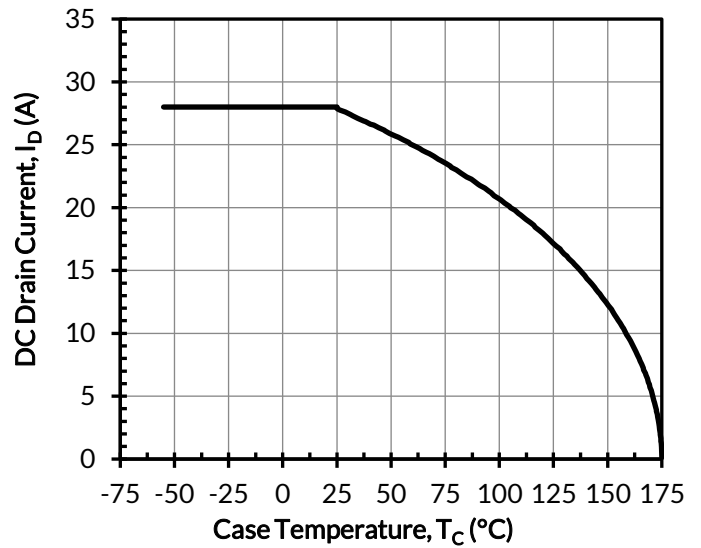


Figure 14. DC drain current derating

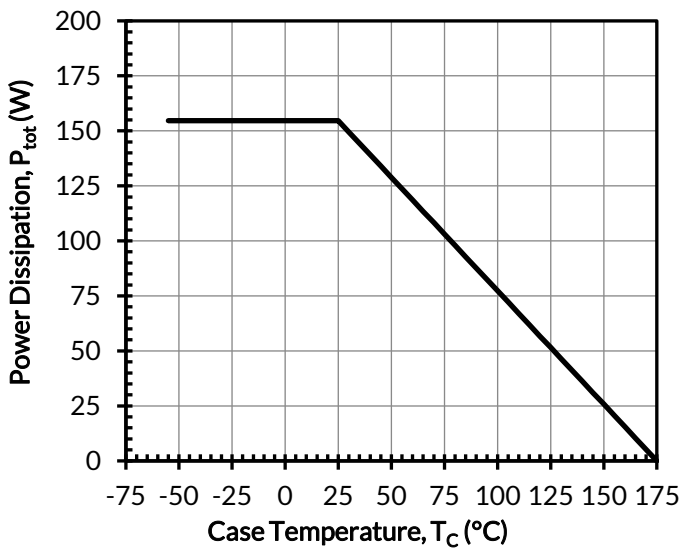


Figure 15. Total power dissipation

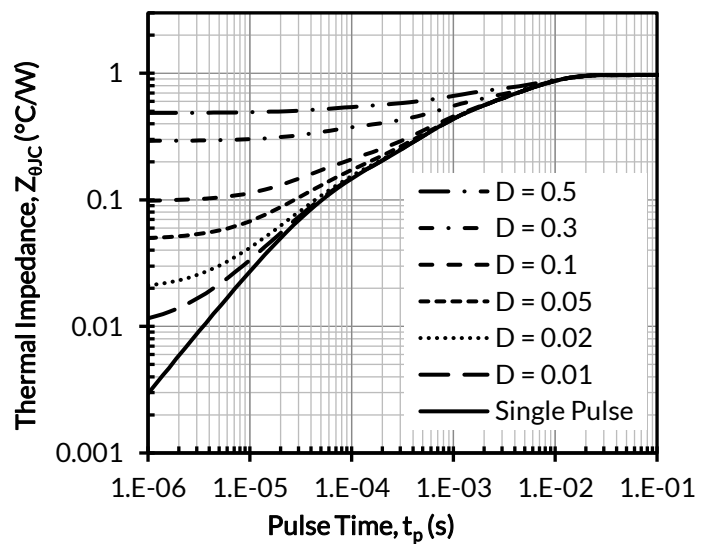


Figure 16. Maximum transient thermal impedance

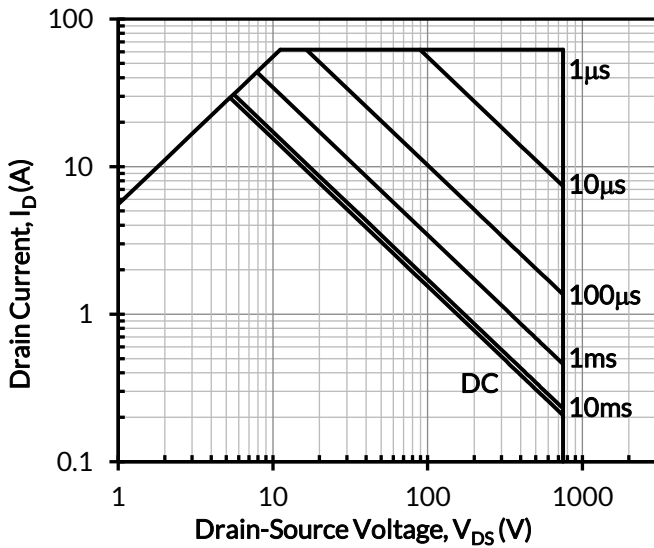


Figure 17. Safe operation area at  $T_C = 25^\circ\text{C}$ ,  $D = 0$ , Parameter  $t_p$

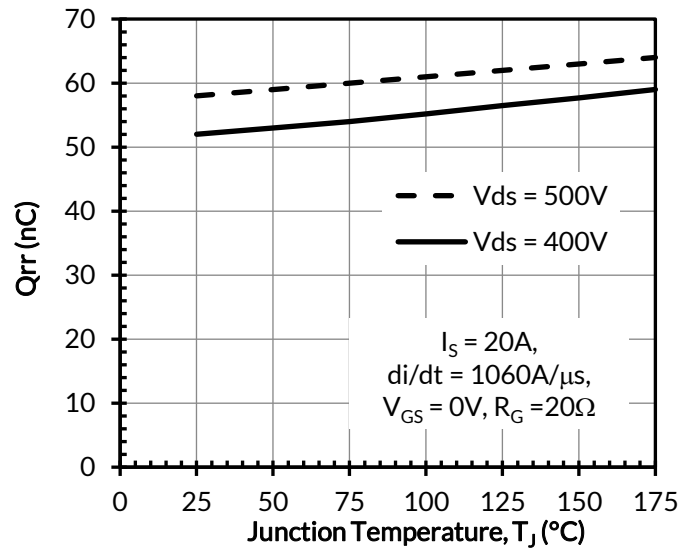


Figure 18. Reverse recovery charge  $Q_{rr}$  vs. junction temperature

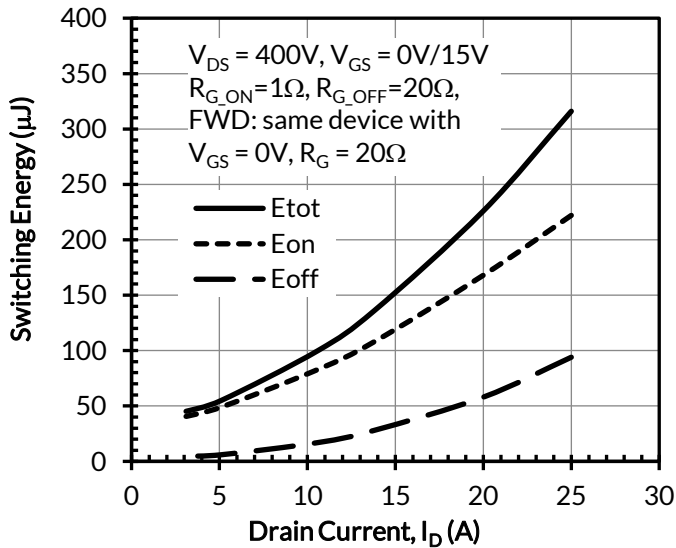


Figure 19. Clamped inductive switching energy vs. drain current at  $V_{DS} = 400\text{V}$  and  $T_J = 25^\circ\text{C}$

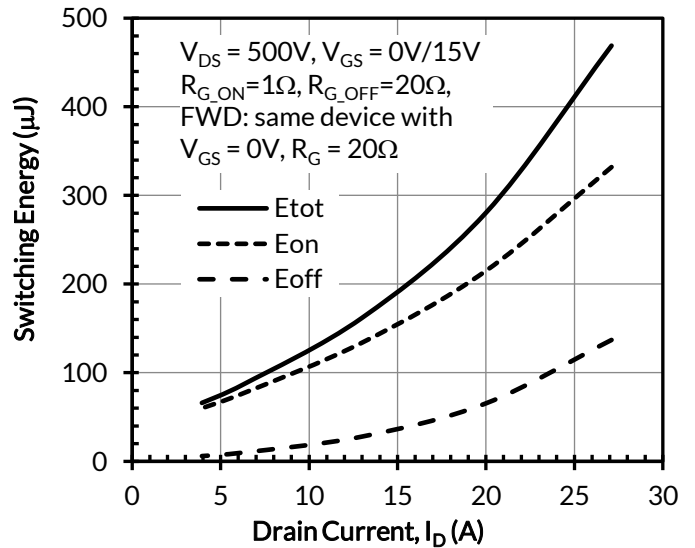


Figure 20. Clamped inductive switching energy vs. drain current at  $V_{DS} = 500\text{V}$  and  $T_J = 25^\circ\text{C}$

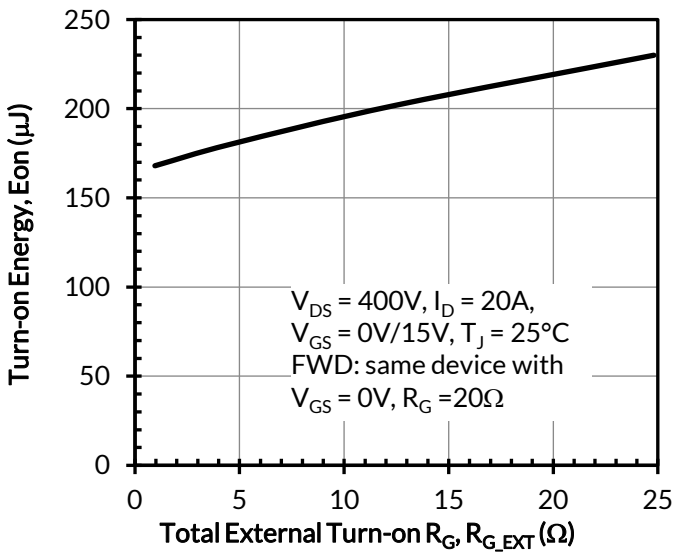


Figure 21. Clamped inductive switching turn-on energy vs.  $R_{G,EXT\_ON}$

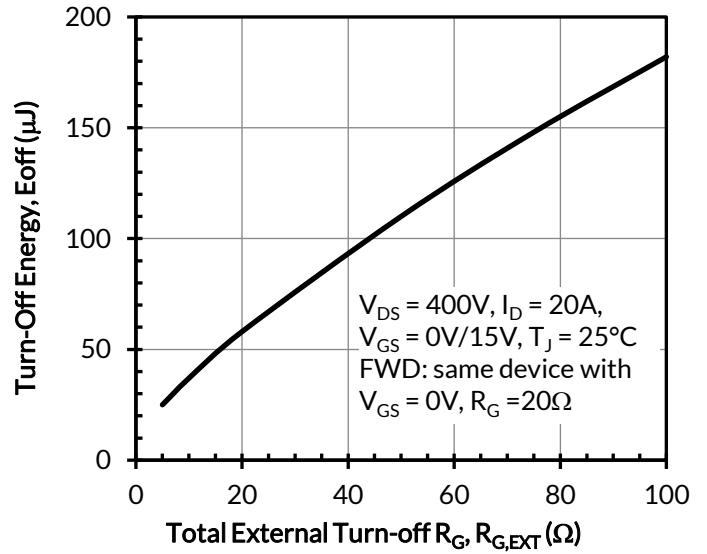


Figure 22. Clamped inductive switching turn-off energy vs.  $R_{G,EXT\_OFF}$

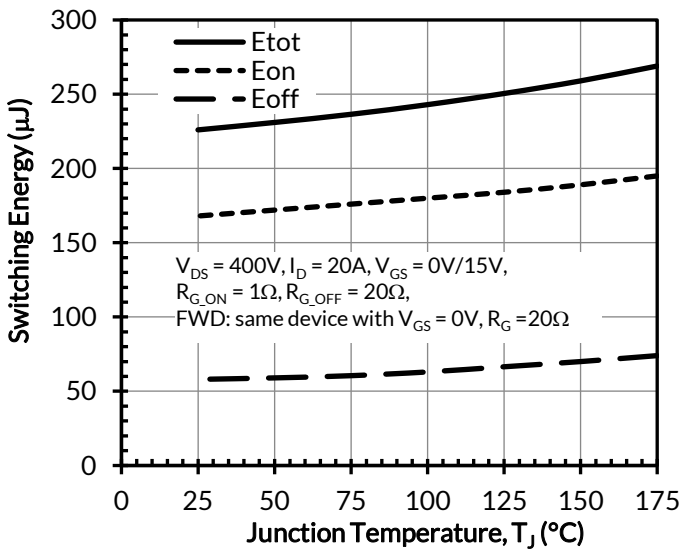


Figure 23. Clamped inductive switching energy vs. junction temperature at  $V_{DS} = 400\text{V}$  and  $I_D = 20\text{A}$

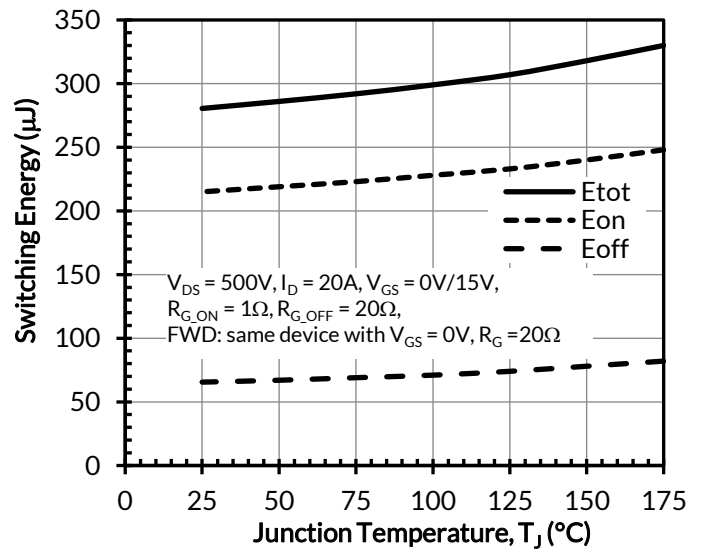


Figure 24. Clamped inductive switching energy vs. junction temperature at  $V_{DS} = 500\text{V}$  and  $I_D = 20\text{A}$

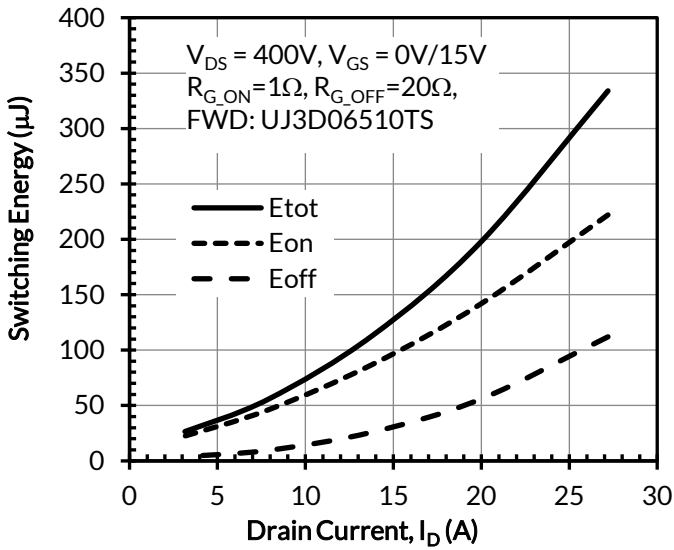


Figure 24. Clamped inductive switching energy vs. drain current at  $V_{DS} = 400V$  and  $T_J = 25^\circ C$

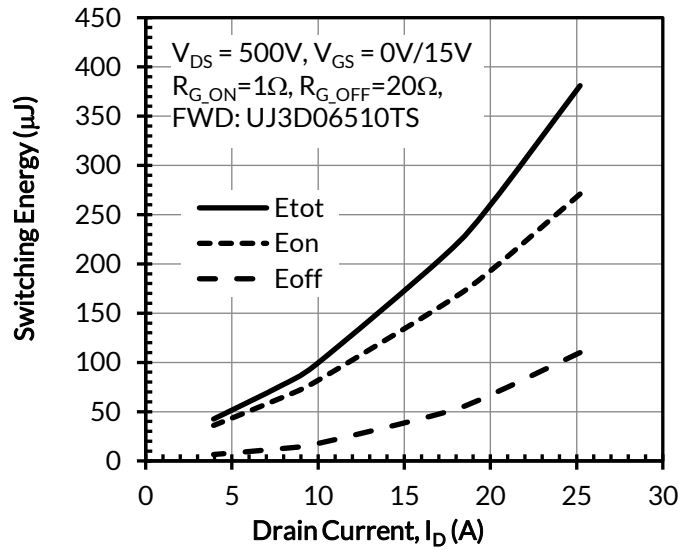


Figure 25. Clamped inductive switching energy vs. drain current at  $V_{DS} = 500V$  and  $T_J = 25^\circ C$

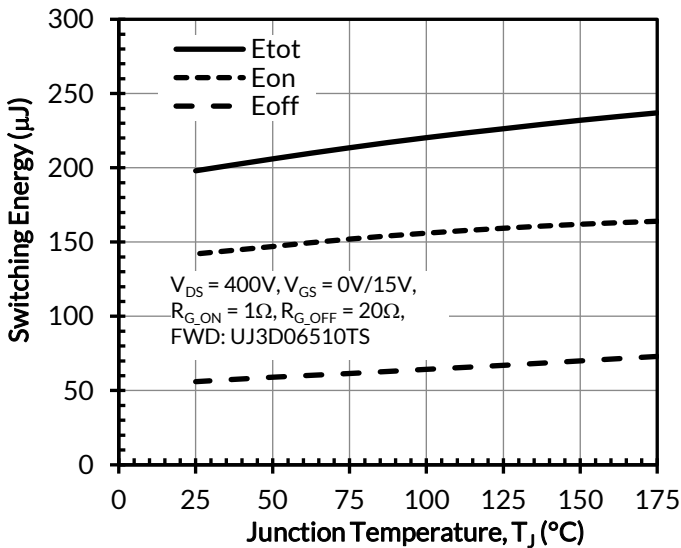


Figure 26. Clamped inductive switching energy vs. junction temperature at  $V_{DS} = 400V$  and  $I_D = 20A$

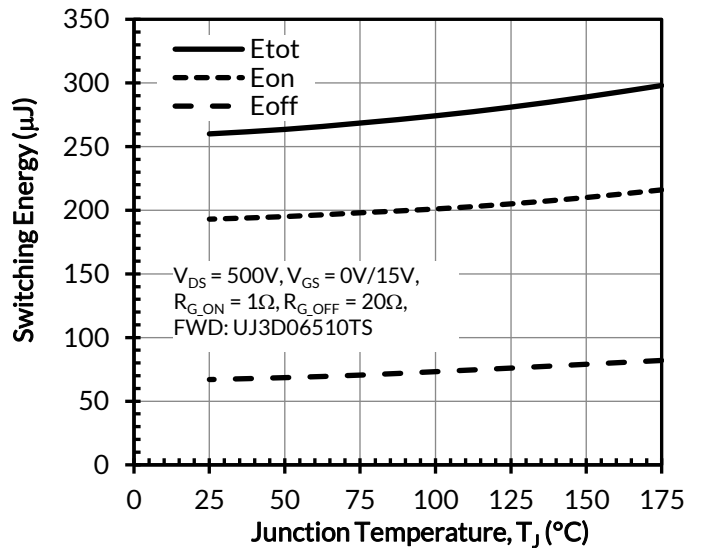


Figure 27. Clamped inductive switching energy vs. junction temperature at  $V_{DS} = 500V$  and  $I_D = 20A$

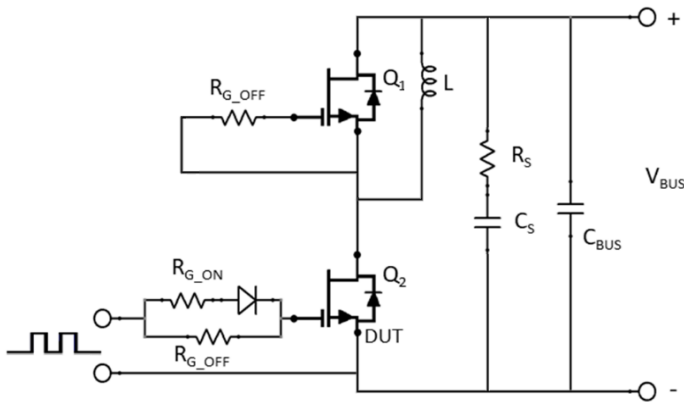


Figure 28. Schematic of the half-bridge mode switching test circuit. Note, a bus RC snubber ( $R_S = 2.5\Omega$ ,  $C_S = 100\text{nF}$ ) is used to reduce the power loop high frequency oscillations.

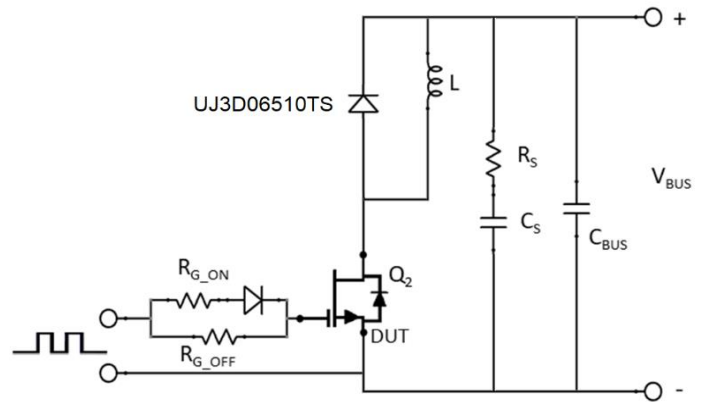


Figure 29. Schematic of the chopper mode switching test circuit. Note, a bus RC snubber ( $R_S = 2.5\Omega$ ,  $C_S = 100\text{nF}$ ) is used to reduce the power loop high frequency oscillations.

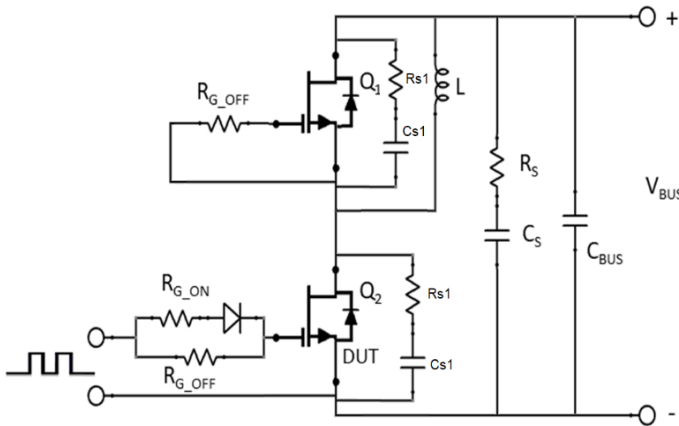


Figure 30. Schematic of the half-bridge mode switching test circuit with device RC snubbers ( $R_{S1} = 10\Omega$ ,  $C_{S1} = 95\text{pF}$ ) and a bus RC snubber ( $R_S = 2.5\Omega$ ,  $C_S = 100\text{nF}$ ).

## Applications Information

SiC FETs are enhancement-mode power switches formed by a high-voltage SiC depletion-mode JFET and a low-voltage silicon MOSFET connected in series. The silicon MOSFET serves as the control unit while the SiC JFET provides high voltage blocking in the off state. This combination of devices in a single package provides compatibility with standard gate drivers and offers superior performance in terms of low on-resistance ( $R_{DS(on)}$ ), output capacitance ( $C_{oss}$ ), gate charge ( $Q_G$ ), and reverse recovery charge ( $Q_{rr}$ ) leading to low conduction and switching losses. The SiC FETs also provide excellent reverse conduction capability eliminating the need for an external anti-parallel diode.

Like other high performance power switches, proper PCB layout design to minimize circuit parasitics is strongly recommended due to the high  $dv/dt$  and  $di/dt$  rates. An external gate resistor is recommended when the FET is working in the diode mode in order to achieve the optimum reverse recovery performance. For more information on SiC FET operation, see [www.unitedsic.com](http://www.unitedsic.com).

A snubber circuit with a small  $R_{(G)}$ , or gate resistor, provides better EMI suppression with higher efficiency compared to using a high  $R_{(G)}$  value. There is no extra gate delay time when using the snubber circuitry, and a small  $R_{(G)}$  will better control both the turn-off  $V_{(DS)}$  peak spike and ringing duration, while a high  $R_{(G)}$  will damp the peak spike but result in a longer delay time. In addition, the total switching loss when using a snubber circuit is less than using high  $R_{(G)}$ , while greatly reducing  $E_{(OFF)}$  from mid-to-full load range with only a small increase in  $E_{(ON)}$ . Efficiency will therefore improve with higher load current. For more information on how a snubber circuit will improve overall system performance, visit the UnitedSiC website at [www.unitedsic.com](http://www.unitedsic.com)

## Disclaimer

UnitedSiC reserves the right to change or modify any of the products and their inherent physical and technical specifications without prior notice. UnitedSiC assumes no responsibility or liability for any errors or inaccuracies within.

Information on all products and contained herein is intended for description only. No license, express or implied, to any intellectual property rights is granted within this document.

UnitedSiC assumes no liability whatsoever relating to the choice, selection or use of the UnitedSiC products and services described herein.

## X-ON Electronics

Largest Supplier of Electrical and Electronic Components

*Click to view similar products for [MOSFET](#) category:*

*Click to view products by [UnitedSiC](#) manufacturer:*

Other Similar products are found below :

[614233C](#) [648584F](#) [IRFD120](#) [JANTX2N5237](#) [2N7000](#) [FCA20N60\\_F109](#) [FDZ595PZ](#) [2SK2545\(Q,T\)](#) [405094E](#) [423220D](#)  
[TPCC8103,L1Q\(CM](#) [MIC4420CM-TR](#) [VN1206L](#) [614234A](#) [715780A](#) [NTNS3166NZT5G](#) [SSM6J414TU,LF\(T](#) [751625C](#)  
[IPS70R2K0CEAKMA1](#) [BUK954R8-60E](#) [DMN3404LQ-7](#) [NTE6400](#) [SQJ402EP-T1-GE3](#) [2SK2614\(TE16L1,Q\)](#) [2N7002KW-FAI](#)  
[DMN1017UCP3-7](#) [EFC2J004NUZTDG](#) [ECH8691-TL-W](#) [FCAB21350L1](#) [P85W28HP2F-7071](#) [DMN1053UCP4-7](#) [NTE221](#) [NTE2384](#)  
[NTE2903](#) [NTE2941](#) [NTE2945](#) [NTE2946](#) [NTE2960](#) [NTE2967](#) [NTE2969](#) [NTE2976](#) [NTE455](#) [NTE6400A](#) [NTE2910](#) [NTE2916](#) [NTE2956](#)  
[NTE2911](#) [US6M2GTR](#) [TK10A80W,S4X\(S](#) [SSM6P69NU,LF](#)